Published in final edited form as:
Mol Pharmacol. 2006 October ; 70(4): 1220–1229. doi:10.1124/mol.106.026823.

Effects of Potent Inhibitors of the Retinoid Cycle on Visual Function and Photoreceptor Protection from Light Damage in Mice[S]

Akiko Maeda, **Tadao Maeda**, **Marcin Golczak**, **Yoshikazu Imanishi**, **Patrick Leahy**, **Ryo Kubota**, and **Krzysztof Palczewski**
Department of Pharmacology (A.M., T.M., M.G., Y.I., K.P.) and Comprehensive Cancer Center (P.L.), Case School of Medicine, Case Western Reserve University, Cleveland, Ohio; and Acucela Inc., Seattle, Washington (R.K.)

Abstract

Regeneration of the chromophore 11-*cis*-retinal is essential for the generation of light-sensitive visual pigments in the vertebrate retina. A deficiency in 11-*cis*-retinal production leads to congenital blindness in humans; however, a buildup of the photoisomerized chromophore can also be detrimental. Such is the case when the photoisomerized all-*trans*-retinal is produced but cannot be efficiently cleared from the internal membrane of the outer segment discs. Sustained increase of all-*trans*-retinal can lead to the formation of toxic condensation products in the eye. Thus, there is a need for potent, selective inhibitors that can regulate the flux of retinoids through the metabolism pathway termed the visual (retinoid) cycle. Here we systematically study the effects of the most potent inhibitor of this cycle, retinylamine (Ret-NH_2), on visual function in mice. Prolonged, sustainable, but reversible suppression of the visual function was observed by Ret-NH_2 as a result of its storage in a prodrug form, *N*-retinylamides. Direct comparison of other inhibitors such as fenretinide and 13-*cis*-retinoic acid showed multiple advantages of Ret-NH_2 and its amides, including a higher potency, specificity, and lower transcription activation. Our results also revealed that mice treated with Ret-NH_2 were completely resistant to the light-induced retina damage. As an experimental tool, Ret-NH_2 allows the replacement of the native chromophore with synthetic analogs in wild-type mice to better understand the function of the chromophore in the activation of rhodopsin and its metabolism through the retinoid cycle.

In the photoreceptors of the vertebrate retina, light causes the isomerization of the visual pigments' chromophore, 11-*cis*-retinylidene, to all-*trans*-retinylidene, followed by the release of all-*trans*-retinal from the opsin binding pocket and its reduction to all-*trans*-retinol (McBee et al., 2001; Lamb and Pugh, 2004; Palczewski, 2006). Vitamin A (all-*trans*-retinol) diffuses to the retinal pigment epithelium (RPE), where it is esterified by lecithin/retinol acyltransferase (LRAT) to all-*trans*-retinyl esters and stored in the retinosomes (Imanishi et al., 2004a,b). All-*trans*-retinyl esters are isomerized to 11-*cis*-retinol in a reaction that involves an abundant 65-kDa RPE-specific protein, termed RPE65, proposed to

[S]The online version of this article (available at http://molpharm.aspetjournals.org) contains supplemental material.

Address correspondence to: Krzysztof Palczewski, Department of Pharmacology, Case Western Reserve University, 10900 Euclid Avenue, R924, Cleveland, OH 44106-4965. kxp65@case.edu.

be retinoid isomerase (Jin et al., 2005; Moiseyev et al., 2005; Redmond et al., 2005). To complete the cycle, 11-*cis*-retinol is then oxidized to its aldehyde. 11-*cis*-Retinal diffuses across the extracellular space to photoreceptors and recombines with opsins to regenerate visual pigments (McBee et al., 2001; Lamb and Pugh, 2004).

The accumulation of fluorescent materials, lipofuscin, in the RPE is associated with aging. In humans, one of the major fluorescent compounds found most prominently in the macula is a pyridinium bis-retinoid, which is derived from two molecules of all-*trans*-retinal and one molecule of phos-phatidylethanolamine, called *N*-retinylidene-*N*-retinyl ethanolamine (A2E) (Parish et al., 1998), which is toxic to the RPE cells. Extensive accumulation of A2E is observed in the recessive juvenile macular degeneration known as the Stargardt disease, caused by mutations in the human ABCR4 gene (Allikmets et al., 1997). ABCR4 is an ATP-binding cassette transporter that localizes to the outer segment (OS) disks of rods and cones, where it is thought to be involved in the transport of *N*-retinylidene-phosphatidylethanolamine (Weng et al., 1999; Beharry et al., 2004). Thus, properly functioning ABCR4 lowers all-*trans*-retinal and consequently decreases the probability of A2E adduct formation. Because it is unknown how to speed up the ABCR4 activity, another strategy proposed by Travis and colleagues was to reduce the flow of retinoids through the inhibition of the visual cycle and thus slow the production of the component of A2E, all-*trans*-retinal (Mata et al., 2000; Radu et al., 2003). The potential inhibitors of the visual cycle include 13-*cis*-retinoic acid (Accutane; Roche) (Radu et al., 2003, 2004a,b), fenretinide (Radu et al., 2005), or various retinoids and farnesyl-containing isoprenoids (TDT and TDH), acting through interaction with RPE65 (Gollapalli and Rando, 2004). The phenotype observed with limited production of 11-*cis*-retinal includes delayed dark adaptation.

Visible light-induced photoreceptor cell damage results from the activation of rhodopsin and culminates in photoreceptor apoptosis. Mice lacking rhodopsin or lacking enzymes involved in the production of rhodopsin's chromophore are completely protected against light-induced apoptosis (Grimm et al., 2000). Prolonged inhibition of the chromophore production by 13-*cis*-retinoic acid protected rats from light damage (Sieving et al., 2001). Thus, inhibition of the visual cycle can be useful in some environmental conditions and can be considered as a treatment of inherited and acquired retinal and macular degeneration.

Positively charged retinoids, all-*trans*-retinylamine (Ret-NH_2), and its isomers are potent inhibitors of the 11-*cis*-retinol production in bovine RPE microsomes (Golczak et al., 2005b). The target for this inhibitor seems to be either a subfraction of RPE65 or another protein essential for the isomerization reaction. We also found that Ret-NH_2 interacts only at micromolar concentrations with retinoic acid receptor and does not activate retinoid X receptor (Golczak et al., 2005b). Moreover, the effect of this inhibitor was remarkably prolonged. This property has been attributed to the fact that Ret-NH_2 is reversibly *N*-*acy*-lated by LRAT to form inactive *N*-retinylamides (Golczak et al., 2005a). The presence of *N*-retinylamides was detected in vivo in wild-type mice supplemented with Ret-NH_2, but not in *Lrat*−/− mice. *N*-Retinylamides are thus the main metabolites of Ret-NH_2 in the liver and the eye and can be mobilized back to Ret-NH_2 by hydrolysis. Mice treated with all-*trans*-Ret-NH_2 showed profound delayed dark adaptation after light exposure.

In this study, we further characterized the properties of all-*trans*-Ret-NH_2 in vivo. We asked how different doses of the inhibitor affect the metabolism of retinoids in the eye; how quickly is all-*trans*-Ret-NH_2 cleared from the eye and other organs; how the efficacy of all-*trans*-Ret-NH_2 compares with the efficacy of its amides and other known inhibitors of the visual cycle; and what are the genes that are activated by treatment with the inhibitor as a indicator of toxicity. We also questioned how all-*trans*-Ret-NH_2 can be used as a research tool; and finally, how all-*trans*-Ret-NH_2 affects light-induced damage of photoreceptors.

Materials and Methods

Animals

All the animal experiments used procedures approved by Case Western Reserve University and conformed to recommendations of the American Veterinary Medical Association Panel on Euthanasia and recommendations of the Association of Research for Vision and Ophthalmology. Animals were maintained in complete darkness or on a 12-h light/dark cycle, and all the manipulations were done under dim red light using a Kodak 1 safelight filter (transmittance >560 nm). Typically, 6-week-old female mice were used in all the experiments. Animals were gavaged with Ret-NH_2 and other retinoids emulsified with 150 μl of vegetable oil as described previously (Van Hooser et al., 2000).

Chemical Synthesis

Ret-NH_2 was prepared according to the published method (Golczak et al., 2005a). *N*-Retinylacetamide and *N*-retinylpalmitamide were prepared by reacting Ret-NH_2 and an excess of acetic anhydride or palmitoyl chloride, respectively, in anhydrous dichloromethane in the presence of *N*,*N*-dimethylaminopyridine at 0°C for 1 h. After the reaction was completed as judged by high-performance liquid chromatography (HPLC), water was added, and the product was extracted with hexane. The hexane layer was washed with saturated NaCl solution, dried with anhydrous magnesium sulfate, filtered, and evaporated in a SpeedVac (Thermo Electron, Waltham, MA). Mass spectral analyses of synthesized retinoids were performed using a Kratos Analytical Instruments (Chestnut Ridge, NY) profile HV-3 direct probe mass spectrometer and electron-impact ionization. 13-*cis*-Retinoic acid and *N*-(4-hydroxy-phenyl)retinamide (fenretinide) were purchased from Sigma or Toronto Research Chemicals Inc.

HPLC Analysis of Retinoids in the Eye

All the experimental procedures related to extraction, derivatization, and separation of retinoids from dissected mouse eyes were carried out under dim red light as described previously (Maeda et al., 2003). Retinoids were separated by normal phase HPLC (Ultrasphere-Si, 4.6 × 250 mm; Beckman Coulter, Fullerton, CA) using 10% ethyl acetate and 90% hexane at a flow rate of 1.4 ml/min with detection at 325 nm using an HP1100 HPLC with a diode array detector and HP Chemstation A.03.03 software.

HPLC Analysis of Ret-NH_2 and Its Amides in the Liver and Blood

Mouse tissues (two eyes, 0.5 g of liver or approximately 0.5 ml of blood) were homogenized and suspended in 3 ml of 20 mM bis-Tris-propane, pH 7.4, containing 50% (v/v) of

methanol. Retinoids were then extracted with 4 ml of hexane. The collected organic phase was evaporated using a SpeedVac, and the retinoids were redis-solved in 400 μl of hexane. Typically, 10 or 100 μl of the liver extract was injected on an HPLC column to detect *N*-retinylamides or Ret-NH_2, respectively. In the case of samples extracted from mouse eyes and blood, the same (100 μl) volume of retinoid solution was injected for *N*-retinylamides and Ret-NH_2 analysis. A normal phase column (Ultrasphere-Si, 5 μm, 4.6 × 250 mm) and a step gradient of ethyl acetate in hexane (10% ethyl acetate for 23 min and then 40% ethyl acetate up to 40 min) at a flow rate of 2 ml/min were used to elute *N*-retinylamides. To detect Ret-NH_2, retinoid separation was performed in 99.5% ethyl acetate containing 0.5% of 7 M ammonia dissolved in methanol.

Liver Retinoic Acid Analysis

Retinoic acid analysis was carried out using methods described previously (Batten et al., 2005). Extracted retinoic acid was injected onto tandem normal phase HPLC columns. The first column was a Varian Microsorb Silica column (3 μm, 4.6 × 100 mm; Varian, Palo Alto, CA), and the second was the Beckman column (Beckman Ultrasphere-Si, 5 μm, 4.6 × 250 mm). An isocratic solvent system of 1000:4.3:0.675 hexane/2-propanol/glacial acetic acid (v/v) was used at a flow rate of 1 ml/min at 20°C with detection at 355 nm calibrated using standards of all-*trans*-retinoic acid and 9-*cis*-retinoic acid purchased from Sigma-Aldrich.

Electroretinograms

Electroretinograms (ERG) were recorded as previously reported (Maeda et al., 2003, 2005). All the experimental procedures were performed under safety light. Dark-adapted mice were anesthetized by i.p. injection using 20 μl/g b.wt. of 6 mg/ml ketamine and 0.44 mg/ml xylazine diluted with 10 mM sodium phosphate, pH 7.2, containing 100 mM NaCl. The pupils were dilated with 0.01% tropicamide. A contact lens electrode was placed on the eye, and a reference electrode and ground electrode were placed in the ear and the tail. ERG were recorded with the universal electrophysiologic system UTAS E-3000 (LKC Technologies, Inc., Gaithers-burg, MD). The light intensity was calibrated by the manufacturer and was computer-controlled. The mice were placed in a Ganzfeld dome, and scotopic and photopic responses to flash stimuli were each obtained from both eyes simultaneously.

Induction and Analysis of Light Damage

Light damage was induced as described previously (Wenzel et al., 2001) with some modifications. Before exposure to light, BALB/c mice (female, 6-week-old) were dark-adapted for 48 h. Light damage was induced in mice without dilated pupils by exposure to 5000 lux of diffuse white fluorescent light (150 W spiral lamp; Commercial Electric, Cleveland, OH) for 2 h (lights on at 11:00 AM). These mice were kept under dark conditions for 7 days and evaluated by ERG, histological study, and rhodopsin measurement.

Histological Study

For light microscopy, mouse eyecups were fixed by immersion in 2.5% glutaraldehyde and 1.6% paraformaldehyde in 0.08 M piperazine-*N*,*N*'-bis(2-ethanesulfonic acid), pH 7.4,

containing 2% sucrose, at room temperature for ~1 h initially and then at 4°C for 24 h. The eyecups were then washed with 0.13 M sodium phosphate, pH 7.3, dehydrated through a CH_3OH series, and embedded in JB4 glycol methacrylate. The sections (6 μm) were stained by immersion with 5% Richardson's stain for 1.5 to 2 min at room temperature and destained in 0.13 M phosphate buffer for 8 to 15 min until the layers could be visualized under a microscope.

Rhodopsin Measurements

Typically, two mouse eyes were used per rhodopsin measurement. Mouse eyes were enucleated and rinsed with water. The lenses were removed, and the eyes were cut into three or four pieces and frozen immediately on a dry ice/ethanol bath. Rhodopsin was extracted with 0.9 ml of 20 mM bis-Tris-propane, pH 7.5, containing 10 mM *n*-dodecyl-β-maltoside and 5 mM freshly neutralized NH_2OH-HCl. The sample was homogenized with a Dounce tissue homogenizer and shaken for 5 min at room temperature. The sample was then centrifuged at 14,000 rpm for 5 min at room temperature. The supernatant was collected, and the pellet was extracted one more time. The combined supernatants were centrifuged at 50,000 rpm for 10 min, and absorption spectra were recorded before and after a 12-min bleach (60 W incandescent bulb). The concentration of rhodopsin was determined by the decrease in absorption at 500 nm using the molar extinction coefficient ε = 42,000 M/cm.

Immunocytochemistry of Arrestin and Transducin α-Subunit

Rabbit anti-arrestin polyclonal antibody was a gift from Dr. G. S. Wu (University of South California, Los Angeles, CA). Mouse anti-transducin α-subunit monoclonal antibody was generated against a 12-amino acid-long peptide corresponding to the C-terminal region of bovine transducin α-subunit coupled to keyhole limpet hemocyanin (K. Palczewski and K. Ridge, unpublished data). Retina sections were incubated in 1.5% normal goat serum in PBST buffer (136 mM NaCl, 11.4 mM sodium phosphate, and 0.1% Triton X-100, pH 7.4) for 15 min at room temperature to block nonspecific labeling, incubated with purified anti-arrestin or anti-transducin α-subunit antibody overnight at 4°C, rinsed with PBST, incubated with indo-carbocyanine (Cy3)-conjugated goat anti-mouse IgG or anti-rabbit IgG, rinsed with PBST, mounted in 50 μl of 2% 1,4-diazabicyclo-2,2,2-octane in 90% glycerol to retard photobleaching, and analyzed under a Leica DM6000 B microscope equipped with a RETIGA EXi CCD camera (QImaging, Burnaby, BC. Canada).

Mouse Treatment for the Array Analysis

Mice were dark adapted for 48 h; gavaged with either 2 μmol of 13-*cis*-retinoic acid, fenretinide, or Ret-NH_2; and kept in the dark for 16 h after the gavage; total RNA was isolated from 10 eyes or from 100 mg of liver of each group with a RiboPure Kit (Ambion, Austin, TX). The quality of the RNA was verified by RNA agarose gel electrophoresis and using the Agilent Bioanalyzer. Aliquots of total RNA isolated from the different tissues and from mice undergoing the various treatments were detection-labeled and hybridized on the mouse genomic microarray using a service provided by NimbleGen System Inc. (Madison, WI). The microarray contained the 37,364 genes and covered the entire mouse transcriptome as represented by the University of California, Santa Cruz database (build HG 17), using a

minimum of 11 probes per gene. The expression of genes was normalized according to probe signal, and the average signal for each gene was normalized for each sample replicate.

Array data for samples across the whole study were normalized by NimbleGen Systems Inc. (Madison, WI), using the robust multichip analysis feature of the data analysis package contained in http://www.bioconductor.org. Project-wide spreadsheets of robust multichip analysis results were exported to Microsoft Excel, and expression level ratios for all the possible pair-wise comparisons, comprising one control and one treated sample, were calculated. These pair-wise ratios were imported to Microsoft Access and mined for credible -fold changes. Changes in gene expression greater than or equal to 2-fold for increases or less than or equal to 0.5-fold for decreases were considered significant. The differentially expressed genes were then exported from Access as Excel files and were annotated using Lucidyx Searcher software (http://www.lucidyx.com).

Results

Effects of Ret-NH_2 on Retinoid Metabolism in the Eye, Blood, and Liver

First, we tested the recovery of 11-*cis*-retinal and the accumulation of esters in the mouse eyes after a treatment with all-*trans*-Ret-NH_2. A wide range of the inhibitor, from 1.75 to 17.5 μmol/treatment, suppressed recovery of more than 80% of the 11-*cis*-retinal level when treated mice were exposed to light (Fig. 1A). Because there are no significant amounts of free 11-*cis*-retinal in the mouse eye, 11-*cis*-retinal is equivalent to the rhodopsin level (Palczewski et al., 1999). In untreated mice, the recovery of full dark adaptation was observed in 24 h (Fig. 1A, inset), whereas on Ret-NH_2 administration, it was slower, reaching 50% of the normal 11-*cis*-retinal level in approximately 3 days for lower doses and approximately 10 days for the 17.5-μmol dose. The highest dose suppressed 11-*cis*-retinal production for as long as 7 days of dark adaptation before recovery was observed (Fig. 1A). To test the suppression of the isomerization reaction during the recovery phase, mice that were treated with 3.5 μmol of the inhibitor and exposed to light after 7 days were examined for recovery of visual chromophore. Under these conditions, during the first 5 h of dark adaptation only 20% of 11-*cis*-retinal was recovered in treated mice, whereas 80% was recovered in control mice (Fig. 1A, inset). These results suggest that the isomerization is still significantly inhibited after 7 days, but because the mice were kept in the dark, 11-*cis*-retinal, albeit produced at a slower rate, was trapped by opsin, which contributed to the observed recovery of the chromophore in these mice.

Second, the all-*trans*-retinyl ester level was elevated in the Ret-NH_2-treated mice proportional to the level of the isomerized chromophore in the eye. Possible transformations involved isomerization of 11-*cis*-retinal to all-*trans*-retinal, reduced to all-*trans*-retinol, and esterified to form all-*trans*-retinyl esters (Fig. 1B). On the other hand, the reduction of the ester levels was proportional to the recovery of 11-*cis*-retinal.

Third, the clearance of Ret-NH_2 and retinylamide after a single dose varying from 1.75 to 17.5 μmol of Ret-NH_2 was measured in the liver, blood, and eye samples (Fig. 2). The level of Ret-NH_2 spiked in 2 h after gavage in all three tissues analyzed and remained stable at low levels throughout the experiment. In the liver, the amide peaked in 3 to 5 days (Fig. 2).

In the eye, faster intake and decay of the amides were observed, whereas in the blood, a spike was only observed 2 h after gavage (Fig. 2). Storage of Ret-NH_2 in the liver and eye facilitates the prolonged effect of this inhibitor in blocking the visual function. Similar results were obtained when mice were treated with *N*-retinylacetamide.

Comparison of the Effect of *N*-retinylacetamide, *N*-retinylpalmitamide, Ret-NH_2, and Other Inhibitors on the Retinoid Cycle

To compare the potency of two other inhibitors of the visual cycle *N*-(4-hydroxyphenyl)retinamide (4-HPR or fenretinide) and 13-*cis*-retinoic acid (Accutane) side by side with Ret-NH_2, *N*-retinylpalmitamide, and *N*-retinylacetamide, mice were gavaged with one of the three select doses of inhibitors, exposed to light, and analyzed 5 and 24 h later after dark adaptation (Fig. 3). For fenretinide and 13-*cis*-retinoic acid, only the highest dose was used. After 5 h, a significant inhibition was observed for Ret-NH_2 > *N*-retinylpalmitamide = *N*-retinylacetamide; after 24 h of dark adaptation, the inhibition was observed only for Ret-NH_2. The analysis of free Ret-NH_2 indicated that the amine was generated from the amide, and the level of the amine decreased with time of dark adaptation and remained only at significant levels for the highest dose (Fig. 3). This observation correlates well with the significant inhibition under these conditions. These results suggest that Ret-NH_2 is the most potent among all the tested inhibitors, implying that the lowest dose will be required to achieve a therapeutic effect compared with other inhibitors, and that the inhibition by Ret-NH_2 has a long-lasting effect. Indeed, the regeneration was suppressed in a dose-dependent manner (Fig. 3). The lower absorption of *N*-retinylamides was observed compared with Ret-NH_2 (M. Golczak and T. Maeda, unpublished data), explaining the significantly reduced efficacy of the amidated form of the inhibitor.

To measure how quickly *N*-retinylacetamide becomes effective in the inhibition of the visual cycle after treatment, mice were exposed to illumination that bleached approximately 50% of rhodopsin. After 2 h of treatment, no inhibition was apparent, but after 4 and 8 h, suppression of *11-cis*-retinal production was observed (Figure S1). A longer period of dark adaptation, approximately 16 h, reduced the effectiveness of the drug, probably because of its being catabolized. As little as 1.75 to 3.5 μmol of *N*-retinylacetamide was sufficient to completely suppress the regeneration reactions in our standard conditions (Figure S2), which was similar to the quantities for Ret-NH_2.

Potential Side Effects on the Visual Cycle Inhibitors

A series of experiments was carried out to assess the potential side effects of Ret-NH_2 in mice. Four treatments with 7-day intervals produced elevated esters 7 days after the last gavage and, as expected, suppressed 11-*cis*-retinal levels, but 2 months after the last gavage the composition of retinoids was normal (Figure S3A). The a-waves and b-waves of the ERG were slightly suppressed in scotopic conditions and significantly suppressed in photopic conditions at high light intensities 7 days after the last gavage, but they recovered completely 2 months later (Figure S3B). Finally, the body weights of multiple treated mice were unchanged compared with the control mice (Figure S3C). We further examined a maintenance dose of Ret-NH_2 that can completely suppress 11-*cis*-retinal production for a long period in dark conditions. When light exposure (~90% rhodopsin bleach) was

performed 4 h after the gavage, gavage of 3.5 μmol of Ret-NH_2 every other day continued inhibiting 11-*cis*-retinal production, whereas a gradual increase of 11-*cis*-retinal was observed in the mice treated with 1.75 μmol of Ret-NH_2 (Figure S4), suggesting that long-term complete blockage of *11-cis*-retinal production can be maintained by multiple gavages of 3.5 μmol of Ret-NH_2.

Ret-NH_2 can be oxidized through retinol, and retinal into retinoic acid. Thus, we next tested the levels of all-*trans*-retinoic acid after the treatment with Ret-NH_2 in mice. Compared with retinol treatment, only a trace elevation of potentially toxic all-*trans*-retinoic acid was detected (Table 1), suggesting that the metabolism of Ret-NH_2 in mice does not lead to elevated formation/accumulation of the ligand for the nuclear hormone receptors.

Retinoic acids are activators of nuclear hormone receptors (Chambon, 1996). Our previous study showed that Ret-NH_2 does not efficiently activate the retinoic acid receptor or retinoid X receptor nuclear hormone receptors in vitro (Golczak et al., 2005b). However, there are a number of nuclear receptors for which the ligand was not identified, and the in vitro study carries obvious risk of over-interpretation. Thus, the expression levels of mRNA were compared between mice treated with 13-*cis*-retinoic acid, fenretinide, and Ret-NH_2 using a 37,364 gene array provided by NimbleGen System Inc. In the liver, 13-*cis*-retinoic acid caused elevated expression, by a factor of 2 or more, of more than 700 genes, as the two other inhibitors produced increases in 345 genes for fenretinide and 367 genes for Ret-NH_2, respectively (Fig. 4). In the liver, 13-*cis*-retinoic acid caused suppression of the expression of more than 3000 genes, and the two other inhibitors decreased expression of 322 genes for fenretinide and 230 genes for Ret-NH_2, respectively (Fig. 4). In the eye, the gene expression pattern was less dramatically changed for 13-*cis*-retinoic acid, whereas fenretinide and Ret-NH_2 had comparable effects as in the liver (Fig. 4). The specific genes whose expressions were the most affected are listed in Tables 1S and 2S of the supplement. In the eye, the increased γ-crystallin protein level was also shown by immunoblotting (Figure S5). A wide range of proteins/enzymes was identified, but not one group of enzymes involved in one specific pathway or transformation seems to be obvious from the analysis. Instead, as expected, a global misregulation of gene expression was observed mostly for 13-*cis*-retinoic acid, whereas Ret-NH_2 and fenretinide had less of an effect on the gene expression. For these two last inhibitors, the pattern of gene expression was similar. Thus, Ret-NH_2 leads to the least amount of altered gene expression patterns compared with other proposed visual cycle inhibitors.

Deficiencies of Arrestin and Transducin α-Subunit Translocation in Ret-NH_2-Administrated Mice

Light-dependent movement of photoreceptor proteins is an essential mechanism of photoreceptor adaptation to the ambient light levels (Sokolov et al., 2002) and could be used to assess the functionality of the phototransduction when the inhibitor is used. Mice treated with Ret-NH_2 showed partial reduction in light-dependent arrestin and rod photoreceptor G protein, transducin, α-subunit translocations. In mice treated with Ret-NH_2, arrestin was localized throughout the photoreceptor cells independent of light conditions (Fig. 5A, right). Slight translocation of arrestin to OS was observed by light adaptation (Fig. 5A, bottom

right), suggesting functional rhodopsin molecules remained at low levels in Ret-NH_2-treated animals. Reduction in transducin movement was also observed in Ret-NH_2-treated mice (Fig. 5B). In the light-adapted retina, OS still retained substantial amounts of transducin α-subunit (Fig. 5B, bottom right). These results indicate that Ret-NH_2 treatment causes deficiency in the light adaptation of rod photoreceptors, most likely by depleting rhodopsin's chromophore.

Substitution of 11-*cis*-Retinal by 9-*cis*-Retinal During the Suppression of the Visual Cycle

During suppression of the regeneration pathway by Ret-NH_2, the visual pigment can be rescued by the exogenous chromophore 9-*cis*-retinal (Fig. 6A). Two doses of Ret-NH_2 were tested as shown in Fig. 6A. Two days after 9-*cis*-retinyl acetate gavage, scotopic and photopic ERG showed significant improvements (Fig. 6B). It is noteworthy that when mice were kept in darkness after regeneration, 9-*cis*-retinal was consequently replaced by naturally produced 11-*cis*-retinal after approximately 2 weeks, thus, in a time course needed for complete renewal of the photoreceptor by phagocytosis (Fig. 6A). These observations suggest that rhodopsin is more stable with 11-*cis*-retinal or that opsin has higher affinity for 11-*cis*-retinal as observed experimentally (Lacy et al., 1984; Kandori et al., 1988). This experiment also shows that Ret-NH_2 does not directly affect recoupling of the chromophore with the opsin.

The Protective Effect of Ret-NH_2 on Light-Induced Retinal Damage in Mice

Mice lacking the active chromophore 11-*cis*-retinal or rhodopsin, *Rpe65*−/− and *Rho*−/− mice, are resistant to light damage (Grimm et al., 2000). These observations suggest that rhodopsin is responsible for light-induced photoreceptor degeneration (Grimm et al., 2000). Five lines of histological, biochemical, and electrophysiological data support the idea that Ret-NH_2 prevents light-induced damage to the eye. First, the histological sections showed that the retinas of the Ret-NH_2-treated mice have fully preserved photoreceptor layers (Fig. 7A) compared with mice not exposed to light. Second, the amount of 11-*cis*-retinal decreased dramatically in mice exposed to light but not among those gavaged with Ret-NH_2 after sufficient dark adaptation (Fig. 7B). Third, rhodopsin levels were considerably diminished to approximately 20% of the control levels. This was not observed when mice were treated with the isomerase inhibitor (Fig. 7C; Table 2). Fourth, immunoblots from mice treated with Ret-NH_2 and exposed to strong illumination showed impressive preservation of rhodopsin (Fig. 7D). Fifth, scotopic and photopic ERG showed preservation of rod- and cone-mediated vision as measured by the a-and b-wave amplitudes under different light intensities (Fig. 7, D–H). Thus, reversible inhibition of the retinoid cycle is an effective way to protect vision from damage caused by intense light.

Discussion

Dose-Dependent, Prolonged, Sustainable, and Reversible Suppression of the Visual Function by Ret-NH_2

Ret-NH_2 is a potent inhibitor of the visual cycle (Golczak et al., 2005a,b; Maeda et al., 2006), with a prolonged mode of action because of its reversible amidation. Thus, the suppression of the visual function depends on the level of the accumulated amides of Ret-

NH_2 (Fig. 2). A single dose of the inhibitor (17.5 μmol) affects production for 11-*cis*-retinal for as long as 8 days (Fig. 1). Bleaching of the visual pigments and conversion of 11-*cis*-retinal to all-*trans*-retinal and subsequently to all-*trans*-retinol led to transient accumulation of all-*trans*-retinyl esters as the retinol formed was quickly esterified (Fig. 1). This blockage in the 11-*cis*-retinal production is reversible because the inhibitor is metabolized to all-*trans*-retinol (Golczak et al., 2005a) and/or secreted (Fig. 2).

No adverse affects were observed during husbandry for multiple gavaged mice for several parameters, including the retinoid content in the eye, visual responses, or body weight (Figure S4). With a proper dose, the 11-*cis*-retinal production could be suppressed for as long as 7 days, the longest period studied here (Figure S4). The metabolism of the inhibitor to retinol is one of the most important toxicological safety features that set it apart from other inhibitors of the visual cycle.

The visual function was mostly investigated by ERG, by regeneration of rhodopsin, and by studying the light-dependent movement of two rod photoreceptor proteins after treatment with the inhibitor. Arrestin and transducin α-subunit are the two most abundant soluble photoreceptor proteins showing massive light-dependent translocation. In the dark-adapted retina, arrestin is localized mostly throughout the photoreceptor cells (Fig. 5A, top left), and the transducin α-subunit is observed specifically in OS (Fig. 5B, top left). On photoactivation of rhodopsin and light adaptation of photoreceptors, arrestin relocates to OS (Fig. 5A, bottom left), and transducin α-subunits move out of the OS (Fig. 5B, bottom left). These results are consistent with the light-dependent translocation of those proteins analyzed by immunoblotting and immunocytochemistry (Sokolov et al., 2002). Currently, two processes are considered to trigger arrestin translocation to OS: 1) passive diffusion and arrestin-rhodopsin interaction and 2) the phototransduction cascade mediated by transducin (Strissel et al., 2006). Although these two possible triggers are distinct, both require rhodopsin. In mice treated with Ret-NH_2 and depleted by photobleaching, no significant movement was observed. These results are consistent with the lack of translocation of arrestin in mice lacking the chromophore because of disruption of the RPE65 gene (Mendez et al., 2003).

Opsin versus Isorhodopsin versus Rhodopsin

Treatment of wild-type mice with Ret-NH_2 paves the way to study visual processes in genetically unmodified mice. The effect of opsin on the cell biology of signal transduction is easily accessible in a precise manner. Detailed studies of the phototransduction became achievable in rod photoreceptors containing different ratios of opsin to rhodopsin. Finally, replacement of the chromophore will allow us to follow the flow (e.g., the isotope-labeled synthetic chromophore) and to investigate how the chromophore modifications affect rhodopsin regeneration (e.g., see Fig. 6). Regeneration of opsin by artificial chromophores would also allow tracking of the integrity and maintenance of photoreceptor OS by a noninvasive spectroscopic approach. Thus, Ret-NH_2 is a promising research tool to study the visual cycle and phototransduction.

Direct Comparison of Ret-NH_2, Its Amides, Fenretinide, and 13-*cis*-Retinoic Acid

Ret-NH_2 seems to be the most potent inhibitor (Golczak et al., 2005b); however, a large proportion of Ret-NH_2 is amidated and inactive in blocking the visual cycle (Fig. 3). Amides are also less efficiently absorbed, further lowering their effective dose. In the condition used, Ret-NH_2 displayed significant levels of inhibition, whereas at the same molar dose, no inhibition of 11-*cis*-retinal regeneration was observed by fenretinide and 13-*cis*-retinoic acid. Thus, Ret-NH_2 is a much more effective inhibitor compared with these other retinoid inhibitors in vivo. When we compared the effects of the expression of eye and liver genes induced by these inhibitors, the strongest activation/inhibition of gene expression was induced by 13-*cis*-retinoic acid, whereas fenretinide and Ret-NH_2 were less active. Taking into account the dose-dependent potency of the inhibition and the longer retention in vivo, Ret-NH_2 has a better safety profile than these other inhibitors.

Complete Protection from the Light Damage

In some conditions, light-induced apoptosis of photoreceptors (Joseph and Li, 1996; Lansel et al., 1998; Organisciak et al., 1998) is triggered by rhodopsin (Grimm et al., 2000). Photoreceptors lacking opsin or rhodopsin are completely protected against light-induced apoptosis, suggesting that rhodopsin is essential for the intracellular death signal induced by light (Grimm et al., 2000). This previous observation is consistent with light damage observed in wild-type mice used in the current study. Inhibition of the chromophore production using Ret-NH_2 in genetically unaltered mice resulted in complete resistance against light-induced photoreceptor damage (Fig. 7; Table 2).

Light damage occurs by at least two distinct pathway (Jacobson and McInnes, 2002), both initiated by rhodopsin. Mice lacking rhodopsin or proteins involved in production of the visual chromophore are resistant to light damage (Grimm et al., 2000). Ret-NH_2 inhibits 11-*cis*-retinal production, resulting in reduction of the amount of rhodopsin that can be activated by light, protecting retinal cells from light damage. One of the potential side effects is delayed dark adaptation, which should not be equated with night blindness because the treated mice recover the visual pigment rhodopsin, albeit more slowly (Fig. 1).

Potential Application to Treat Human Eye Diseases

The most exciting aspect of the study is the potential application of Ret-NH_2 for treatment of A2E–accumulating ocular diseases. Accumulation of A2E, which is toxic for the RPE, has been proposed to be an etiologic factor not only for Stargardt disease (Weng et al., 1999; Mata et al., 2000, 2001) but also for age-related macular degenerations (Mata et al., 2000). Inhibiting A2E formation should therefore slow the progression of visual loss in diseases associated with A2E overaccumulation. Thus, the current study is an important prelude for understanding the metabolism, the proper doses, timing, and mechanism of the drug action. Critically important is the reversibility of the visual suppression and restoration of normal retinoid content after treatment. Ret-NH_2 can also be applied to prevent the light-mediated retina damage (e.g., extensive light exposure from endoillumination sources during prolonged retina surgery).

Supplementary Material

Refer to Web version on PubMed Central for supplementary material.

Acknowledgments

We thank Dr. A. R. Moise for help with the gene array experiments and Melissa Puffenbarger for help with manuscript preparation. We thank Drs. N. Rao and G. S. Wu for providing the arrestin antibody and Drs. R. Tzekov and A. R. Moise for the comments on the manuscript.

This research was supported by National Institutes of Health grant EY09339 and P30-EY11373, and a grant from National Neurovision Research Institute (A.M.). This research was supported by the Gene Expression and Genotyping Facility of the Comprehensive Cancer Center of Case Western Reserve University and University Hospitals of Cleveland (P30-CA43703).

University of Washington and Acucela Inc. may commercialize some of the technology described in this work. K.P. is a consultant for Acucela Inc.

ABBREVIATIONS

RPE	retinal pigment epithelium
LRAT	lecithin/retinol acyltransferase
RPE65	an RPE-specific 65 kDa protein
A2E	*N*-retinylidene-*N*-retinyl ethanolamine
OS	outer segment
Ret-NH$_2$	retinylamine
HPLC	high-performance liquid chromatography
ERG	electro-retinogram(s)
PBST	phosphate-buffered saline/Triton X-100

References

Allikmets R, Singh N, Sun H, Shroyer NF, Hutchinson A, Chidambaram A, Gerrard B, Baird L, Stauffer D, Peiffer A, et al. A photoreceptor cell-specific ATP-binding transporter gene (ABCR) is mutated in recessive Stargardt macular dystrophy. Nat Genet. 1997; 15:236–246. [PubMed: 9054934]

Batten ML, Imanishi Y, Tu DC, Doan T, Zhu L, Pang J, Glushakova L, Moise AR, Baehr W, Van Gelder RN, et al. Pharmacological and rAAV gene therapy rescue of visual functions in a blind mouse model of leber congenital amaurosis. PLoS Med. 2005; 2:e333. [PubMed: 16250670]

Beharry S, Zhong M, Molday RS. N-retinylidene-phosphatidylethanolamine is the preferred retinoid substrate for the photoreceptor-specific ABC transporter ABCA4 (ABCR). J Biol Chem. 2004; 279:53972–53979. [PubMed: 15471866]

Chambon P. A decade of molecular biology of retinoic acid receptors. FASEB J. 1996; 10:940–954. [PubMed: 8801176]

Golczak M, Imanishi Y, Kuksa V, Maeda T, Kubota R, Palczewski K. Lecithin:retinol acyltransferase is responsible for amidation of retinylamine, a potent inhibitor of the retinoid cycle. J Biol Chem. 2005a; 280:42263–42273. [PubMed: 16216874]

Golczak M, Kuksa V, Maeda T, Moise AR, Palczewski K. Positively charged retinoids are potent and selective inhibitors of the trans-cis isomerization in the retinoid (visual) cycle. Proc Natl Acad Sci USA. 2005b; 102:8162–8167. [PubMed: 15917330]

Gollapalli DR, Rando RR. The specific binding of retinoic acid to RPE65 and approaches to the treatment of macular degeneration. Proc Natl Acad Sci USA. 2004; 101:10030–10035. [PubMed: 15218101]

Grimm C, Wenzel A, Hafezi F, Yu S, Redmond TM, Reme CE. Protection of Rpe65-deficient mice identifies rhodopsin as a mediator of light-induced retinal degeneration. Nat Genet. 2000; 25:63–66. [PubMed: 10802658]

Imanishi Y, Batten ML, Piston DW, Baehr W, Palczewski K. Noninvasive two-photon imaging reveals retinyl ester storage structures in the eye. J Cell Biol. 2004a; 164:373–383. [PubMed: 14745001]

Imanishi Y, Gerke V, Palczewski K. Retinosomes: new insights into intracellular managing of hydrophobic substances in lipid bodies. J Cell Biol. 2004b; 166:447–453. [PubMed: 15314061]

Jacobson SG, McInnes RR. Blinded by the light. Nat Genet. 2002; 32:215–216. [PubMed: 12355075]

Jin M, Li S, Moghrabi WN, Sun H, Travis GH. Rpe65 is the retinoid isomerase in bovine retinal pigment epithelium. Cell. 2005; 122:449–459. [PubMed: 16096063]

Joseph RM, Li T. Overexpression of Bcl-2 or Bcl-XL transgenes and photoreceptor degeneration. Investig Ophthalmol Vis Sci. 1996; 37:2434–2446. [PubMed: 8933760]

Kandori H, Matuoka S, Nagai H, Shichida Y, Yoshizawa T. Dependency of apparent relative quantum yield of isorhodopsin to rhodopsin on the photon density of picosecond laser pulse. Photochem Photobiol. 1988; 48:93–97. [PubMed: 3217445]

Lacy ME, Veronee CD, Crouch RK. Regeneration of rhodopsin and isorhodopsin in rod outer segment preparations: absence of effect of solvent parameters. Physiol Chem Phys Med NMR. 1984; 16:275–281. [PubMed: 6240663]

Lamb TD, Pugh EN Jr. Dark adaptation and the retinoid cycle of vision. Prog Retin Eye Res. 2004; 23:307–380. [PubMed: 15177205]

Lansel N, Hafezi F, Marti A, Hegi M, Reme C, Niemeyer G. The mouse ERG before and after light damage is independent of p53. Doc Ophthalmol. 1998; 96:311–320. [PubMed: 10855807]

Maeda A, Maeda T, Imanishi Y, Golczak M, Moise AR, Palczewski K. Aberrant metabolites in mouse models of congenital blinding diseases: formation and storage of retinyl esters. Biochemistry. 2006; 45:4210–4219. [PubMed: 16566595]

Maeda A, Maeda T, Imanishi Y, Kuksa V, Alekseev A, Bronson JD, Zhang H, Zhu L, Sun W, Saperstein DA, et al. Role of photoreceptor-specific retinol dehydrogenase in the retinoid cycle in vivo. J Biol Chem. 2005; 280:18822–18832. [PubMed: 15755727]

Maeda T, Van Hooser JP, Driessen CA, Filipek S, Janssen JJ, Palczewski K. Evaluation of the role of the retinal G protein-coupled receptor (RGR) in the vertebrate retina in vivo. J Neurochem. 2003; 85:944–956. [PubMed: 12716426]

Mata NL, Tzekov RT, Liu X, Weng J, Birch DG, Travis GH. Delayed dark-adaptation and lipofuscin accumulation in abcr+/− mice: implications for involvement of ABCR in age-related macular degeneration. Investig Ophthalmol Vis Sci. 2001; 42:1685–1690. [PubMed: 11431429]

Mata NL, Weng J, Travis GH. Biosynthesis of a major lipofuscin fluorophore in mice and humans with ABCR-mediated retinal and macular degeneration. Proc Natl Acad Sci USA. 2000; 97:7154–7159. [PubMed: 10852960]

McBee JK, Palczewski K, Baehr W, Pepperberg DR. Confronting complexity: the interlink of phototransduction and retinoid metabolism in the vertebrate retina. Prog Retin Eye Res. 2001; 20:469–529. [PubMed: 11390257]

Mendez A, Lem J, Simon M, Chen J. Light-dependent translocation of arrestin in the absence of rhodopsin phosphorylation and transducin signaling. J Neurosci. 2003; 23:3124–3129. [PubMed: 12716919]

Moiseyev G, Chen Y, Takahashi Y, Wu BX, Ma JX. RPE65 is the isomerohydrolase in the retinoid visual cycle. Proc Natl Acad Sci USA. 2005; 102:12413–12418. [PubMed: 16116091]

Organisciak DT, Darrow RM, Barsalou L, Darrow RA, Kutty RK, Kutty G, Wiggert B. Light history and age-related changes in retinal light damage. Investig Ophthalmol Vis Sci. 1998; 39:1107–1116. [PubMed: 9620069]

Palczewski K. G protein-coupled receptor rhodopsin. Annu Rev Biochem. 2006; 75:743–767. [PubMed: 16756510]

Palczewski K, Van Hooser JP, Garwin GG, Chen J, Liou GI, Saari JC. Kinetics of visual pigment regeneration in excised mouse eyes and in mice with a targeted disruption of the gene encoding interphotoreceptor retinoid-binding protein or arrestin. Biochemistry. 1999; 38:12012–12019. [PubMed: 10508404]

Parish CA, Hashimoto M, Nakanishi K, Dillon J, Sparrow J. Isolation and one-step preparation of A2E and iso-A2E, fluorophores from human retinal pigment epithelium. Proc Natl Acad Sci USA. 1998; 95:14609–14613. [PubMed: 9843937]

Radu RA, Han Y, Bui TV, Nusinowitz S, Bok D, Lichter J, Widder K, Travis GH, Mata NL. Reductions in serum vitamin A arrest accumulation of toxic retinal fluorophores: a potential therapy for treatment of lipofuscin-based retinal diseases. Investig Ophthalmol Vis Sci. 2005; 46:4393–4401. [PubMed: 16303925]

Radu RA, Mata NL, Bagla A, Travis GH. Light exposure stimulates formation of A2E oxiranes in a mouse model of Stargardt's macular degeneration. Proc Natl Acad Sci USA. 2004a; 101:5928–5933. [PubMed: 15067110]

Radu RA, Mata NL, Nusinowitz S, Liu X, Sieving PA, Travis GH. Treatment with isotretinoin inhibits lipofuscin accumulation in a mouse model of recessive Stargardt's macular degeneration. Proc Natl Acad Sci USA. 2003; 100:4742–4747. [PubMed: 12671074]

Radu RA, Mata NL, Nusinowitz S, Liu X, Travis GH. Isotretinoin treatment inhibits lipofuscin accumulation in a mouse model of recessive Stargardt's macular degeneration. Novartis Found Symp. 2004b; 255:51–63. discussion 63–57, 177–178. [PubMed: 14750596]

Redmond TM, Poliakov E, Yu S, Tsai JY, Lu Z, Gentleman S. Mutation of key residues of RPE65 abolishes its enzymatic role as isomerohydrolase in the visual cycle. Proc Natl Acad Sci USA. 2005; 102:13658–13663. [PubMed: 16150724]

Sieving PA, Chaudhry P, Kondo M, Provenzano M, Wu D, Carlson TJ, Bush RA, Thompson DA. Inhibition of the visual cycle in vivo by 13-cis retinoic acid protects from light damage and provides a mechanism for night blindness in isotretinoin therapy. Proc Natl Acad Sci USA. 2001; 98:1835–1840. [PubMed: 11172037]

Sokolov M, Lyubarsky AL, Strissel KJ, Savchenko AB, Govardovskii VI, Pugh EN Jr, Arshavsky VY. Massive light-driven translocation of transducin between the two major compartments of rod cells: a novel mechanism of light adaptation. Neuron. 2002; 34:95–106. [PubMed: 11931744]

Strissel KJ, Sokolov M, Trieu LH, Arshavsky VY. Arrestin translocation is induced at a critical threshold of visual signaling and is superstoichiometric to bleached rhodopsin. J Neurosci. 2006; 26:1146–1153. [PubMed: 16436601]

Van Hooser JP, Aleman TS, He YG, Cideciyan AV, Kuksa V, Pittler SJ, Stone EM, Jacobson SG, Palczewski K. Rapid restoration of visual pigment and function with oral retinoid in a mouse model of childhood blindness. Proc Natl Acad Sci USA. 2000; 97:8623–8628. [PubMed: 10869443]

Weng J, Mata NL, Azarian SM, Tzekov RT, Birch DG, Travis GH. Insights into the function of Rim protein in photoreceptors and etiology of Stargardt's disease from the phenotype in abcr knockout mice. Cell. 1999; 98:13–23. [PubMed: 10412977]

Wenzel A, Reme CE, Williams TP, Hafezi F, Grimm C. The Rpe65 Leu450Met variation increases retinal resistance against light-induced degeneration by slowing rhodopsin regeneration. J Neurosci. 2001; 21:53–58. [PubMed: 11150319]

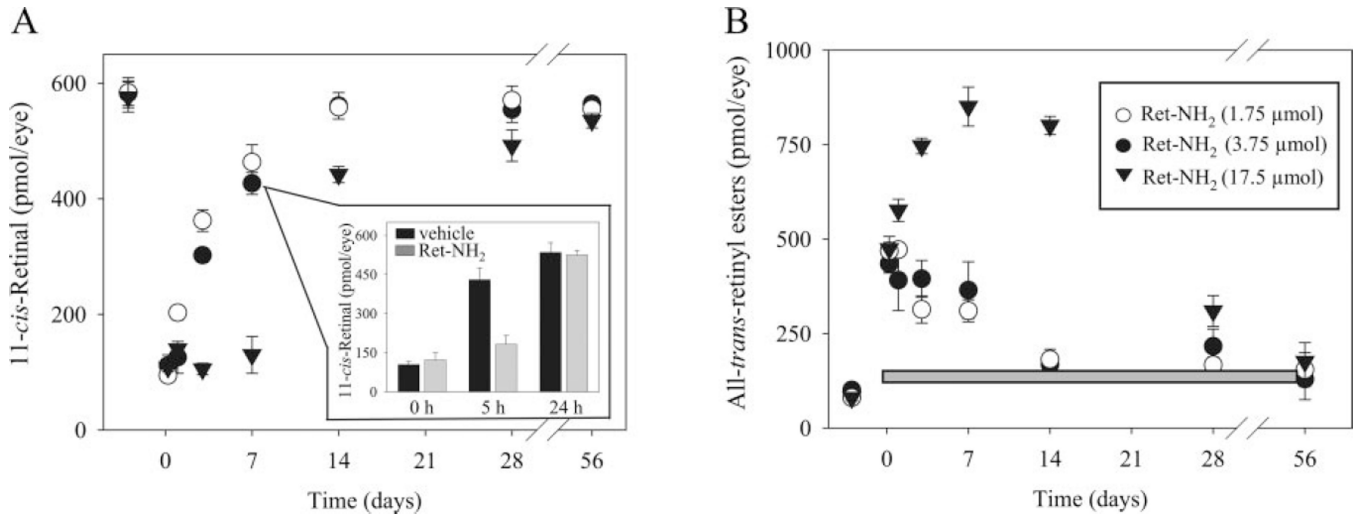

Fig. 1.

Effects of different doses of Ret-NH_2 on the 11-*cis*-retinal and all-*trans*-retinyl ester levels in the eye. The 48-h dark-adapted C57BL/6 mice were gavaged with a single dose of Ret-NH_2 (1.75, 3.5, or 17.5 μmol). Next, 24 h after gavage, the mice were exposed to background light at 150 cd/m^2 for 20 min. Retinoid levels, 11-*cis*-retinal (A) and all-*trans*-retinyl ester (B), in the eye were examined at various times of dark adaptation. Retinoids were analyzed using HPLC methods as described under *Materials and Methods*. Inset, subset of mice gavaged with 3.5 μmol of Ret-NH_2 were exposed a second time to the same intensity of illumination 7 days after the first exposure to light. All the procedures were carried out in the dark. The gray bar indicates the levels of all-*trans*-retinyl esters in wild-type mice. Mean ± S.D. was indicated (*n*= 3 for each point).

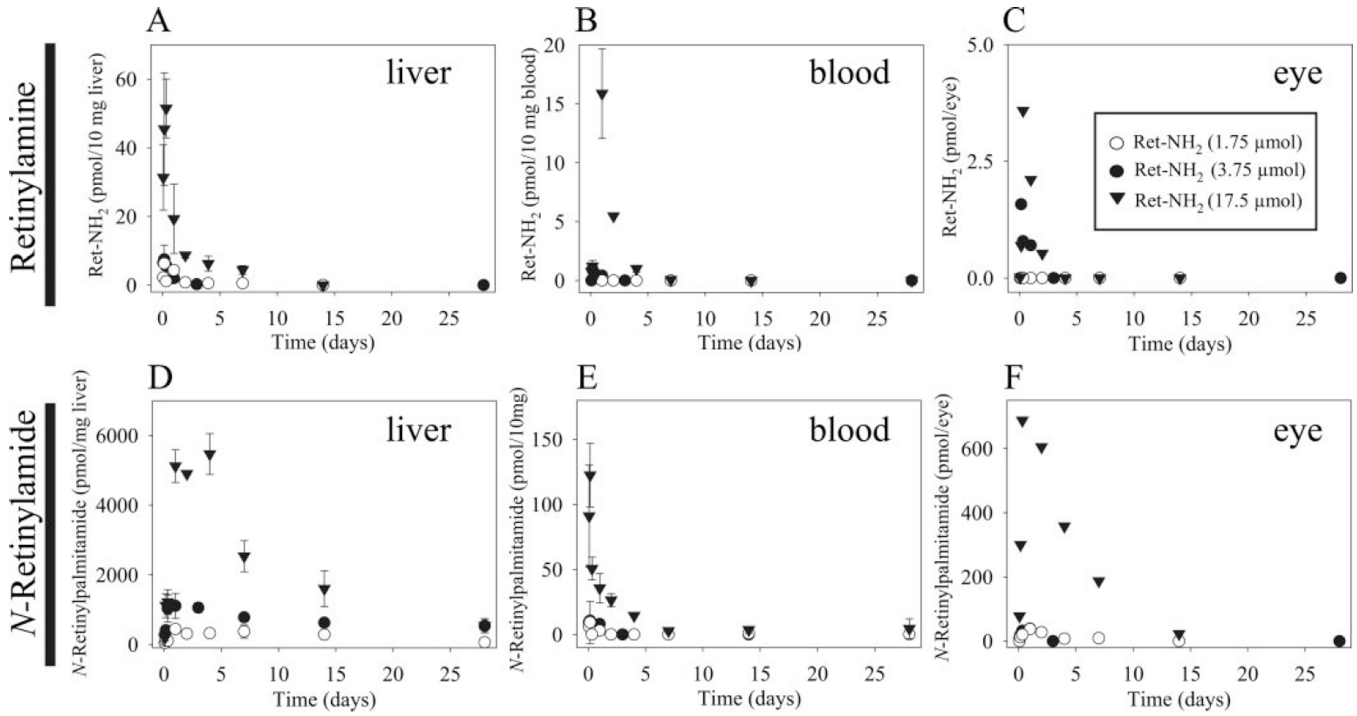

Fig. 2.

Clearance of Ret-NH_2 in the liver, blood, and eye. The 48-h dark-adapted C57BL/6 mice were gavaged with a single dose of Ret-NH_2 (1.75, 3.5, or 17.5 µmol). After gavage, the levels of Ret-NH_2 and *N*-retinylpalmitamide were measured in the liver (A, D), blood (B, E), and eye (C, F) at various time points. Retinoids were analyzed using HPLC methods as described under *Materials and Methods*. Mean ± S.D. was indicated (*n*= 3 for each point).

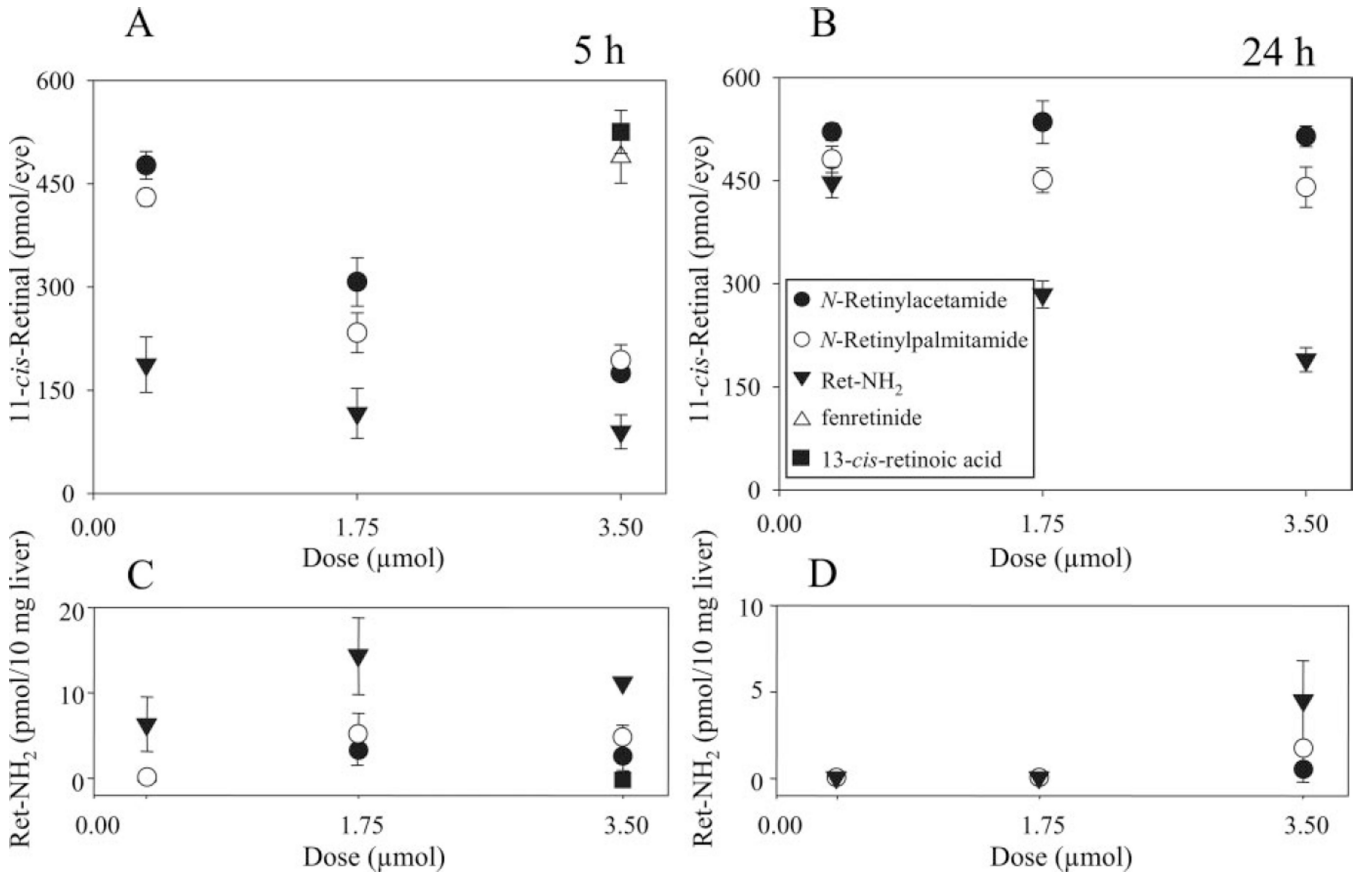

Fig. 3.

Comparison of the effect of Ret-NH_2 and other inhibitors on the retinoid cycle. The 48-h dark-adapted C57BL/6 mice were gavaged with a single dose of *N*-retinylamides, Ret-NH_2, fenretinide, or 13-*cis*-retinoic acid (0.35,1.75, or 3.5 μmol). The mice were exposed to background light at 150 cd/m^2 for 20 min at 24 h after gavage. The 11-*cis*-retinal in the eye and Ret-NH_2 in the liver were analyzed at 5 h (A; eye) (C; liver) and 24 h (B; eye) (D; liver) after the bleach. Retinoids were analyzed using HPLC methods as described under *Materials and Methods*. Mean ± S.D. was indicated (*n*= 3 for each point).

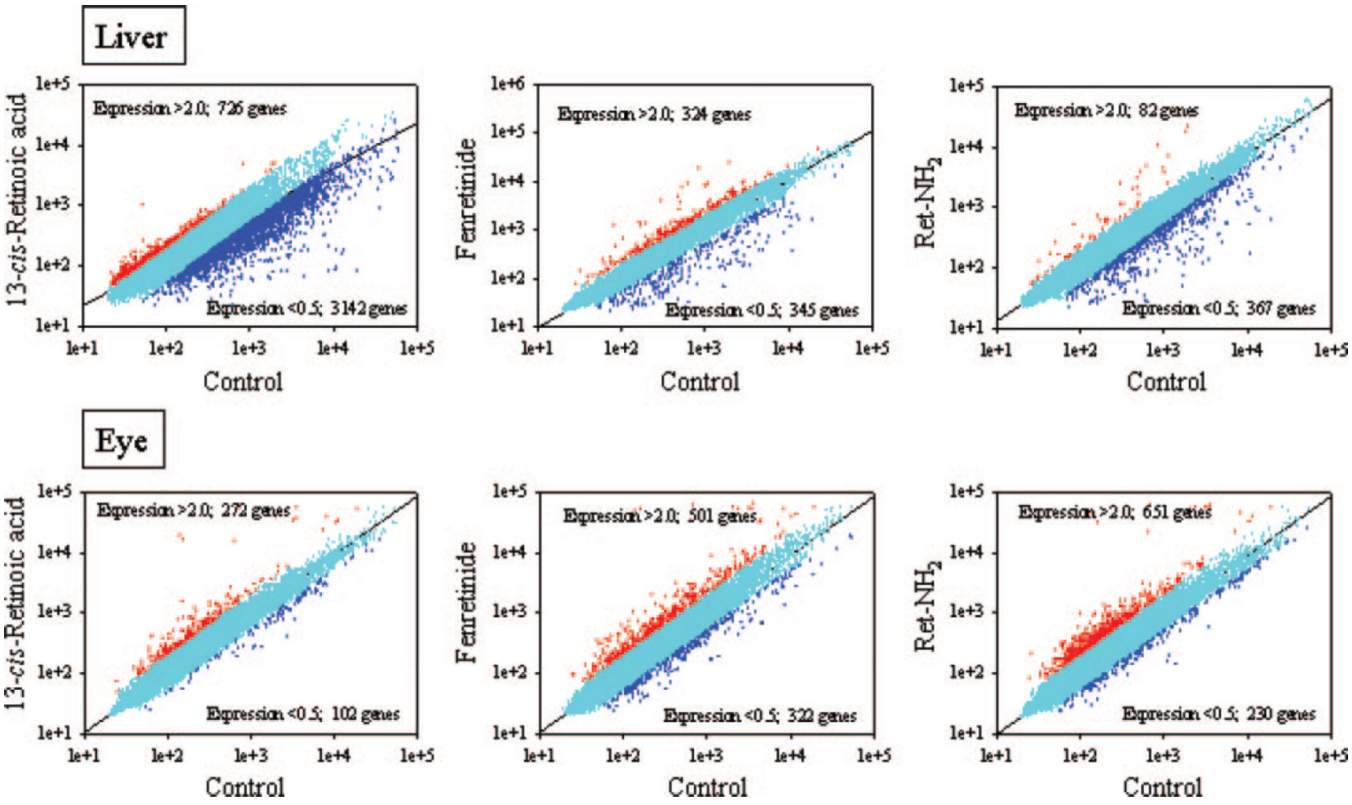

Fig. 4.

Gene array analysis. The expression levels of mRNA were compared between mice treated with 13-*cis*-retinoic acid, fenretinide, and Ret-NH_2 using a 37,364 cDNA array (provided by NimbleGen System Inc.) as described under *Materials and Methods*. Normalized values of mRNA expression were plotted, control versus each treated group for liver mRNA (top) and for eye mRNA (bottom) as scattered plot with Sigma Plot v.9.0. Numbers of genes for which expression level was changed to less than 0.5 of control (dark blue points) or to more than 2 after the treatment (red points) were indicated, whereas the levels of expression within the experimental error is shown in light blue.

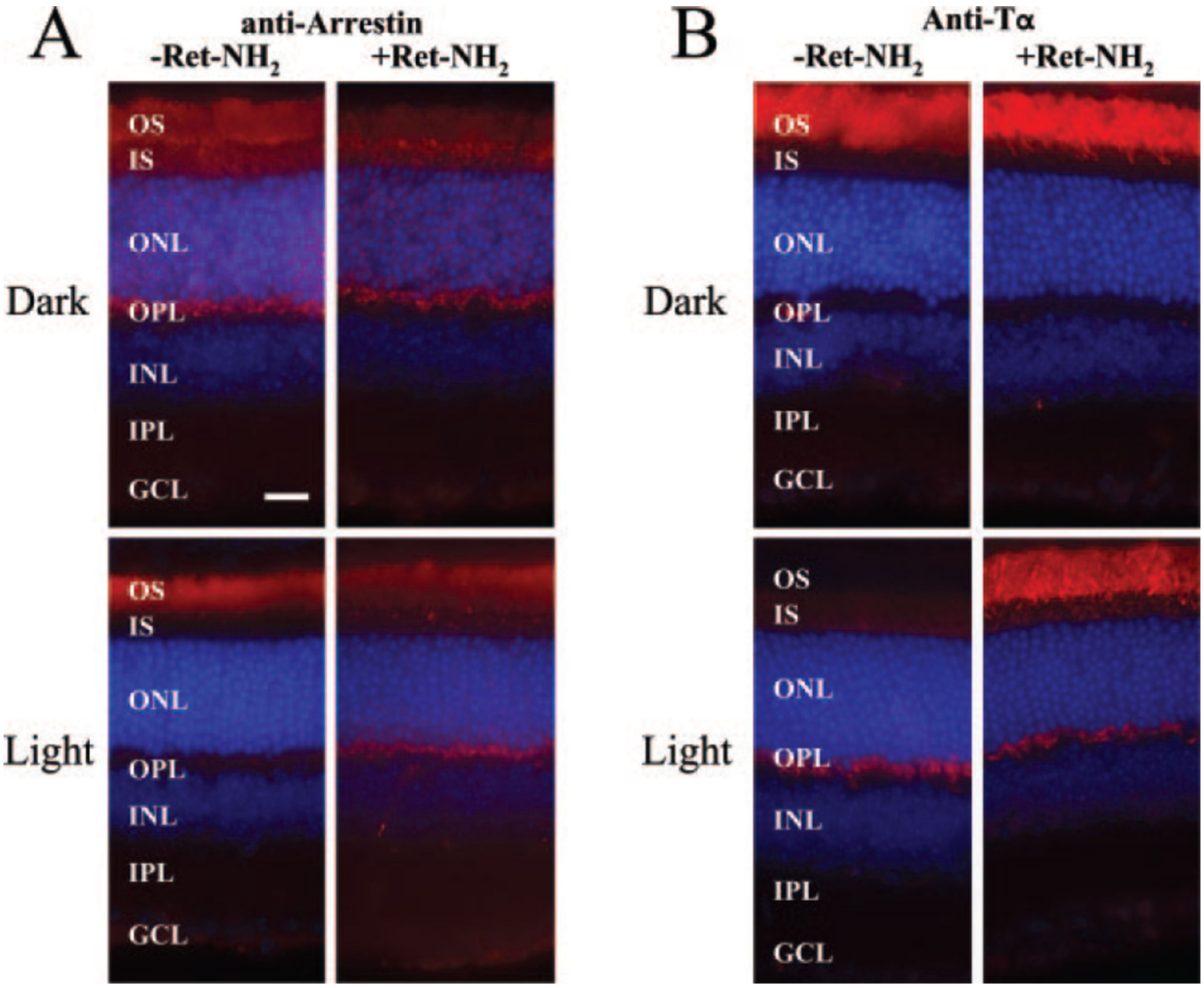

Fig. 5.

Deficiencies of arrestin and transducin a-subunit translocation in Ret-NH_2-treated mice. Left column indicates the mice without Ret-NH_2 administration, and right column shows the mice gavaged with Ret-NH_2. A, immunofluorescent localization of rod arrestin (red). In the dark adapted retinas, arrestin was distributed throughout the retina. Under light-adapted conditions, translocation of arrestin to photoreceptor OS was observed in control mice (left, bottom). Only minimal translocation of arrestin to OS was observed in light-adapted mice gavaged with Ret-NH_2. B, immunofluorescent localization of transducin α-subunit (red). In the dark-adapted retinas, transducin α is localized in photoreceptor OS. In light-adapted retinas of control mice (bottom left), transducin is localized in IS, ONL, and OPL. This light-dependent translocation is mostly abolished in mice gavaged with Ret-NH_2, which shows the transducin α immunoreactivity mostly in OS and weakly in OPL. IS, inner segment; ONL, outer nuclear layer; OPL, outer plexiform layer; INL, inner nuclear layer; IPL, inner plexiform layer; GCL, ganglion cell layer. Nuclei are stained with Hoechst 33342 (blue).

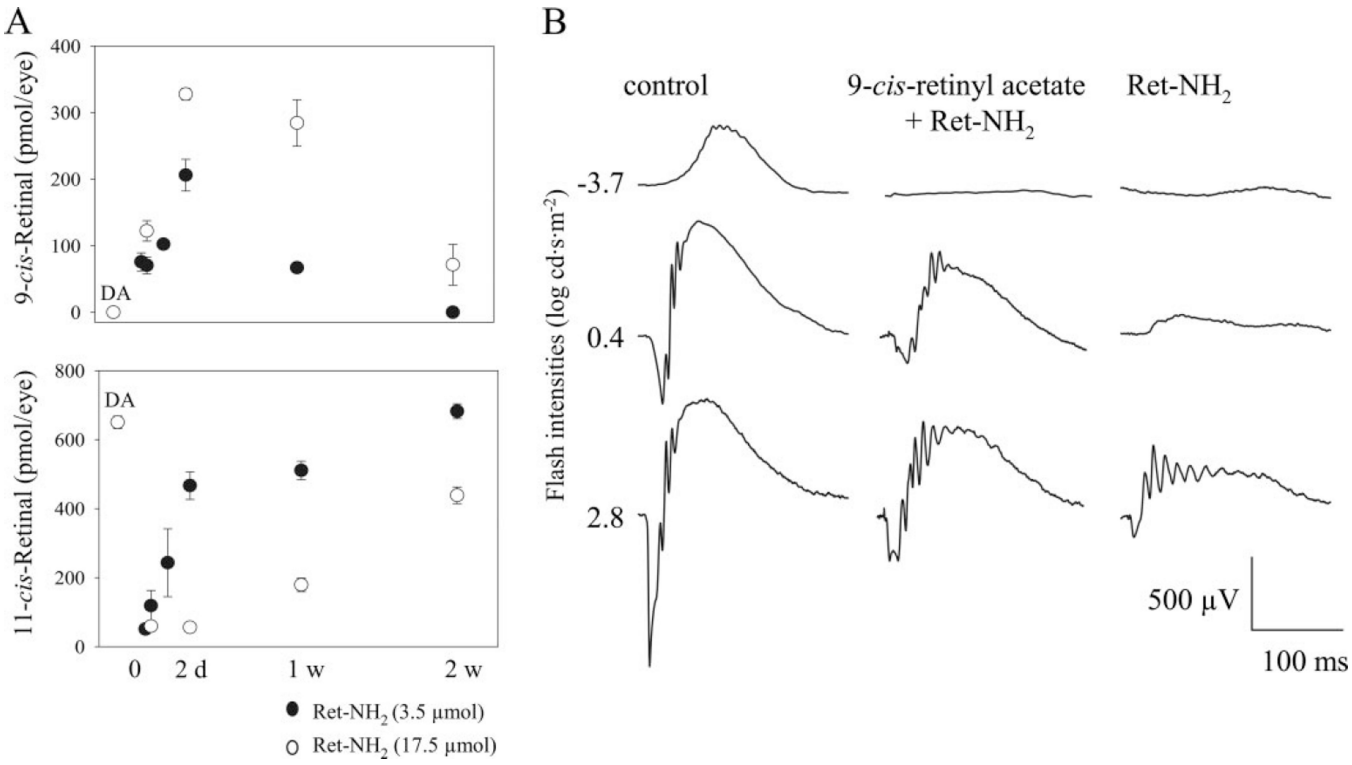

Fig. 6.

Substitution of 11-*cis*-retinal by 9-*cis*-retinal. The 48-h dark-adapted C57BL/6 mice were gavaged once with Ret-NH_2 (3.5 or 17.5 µmol), and 16 h after gavage the mice were exposed to background light at 500 cd/m^2 for 24 min. Next, mice were placed in the dark and 2 h after exposure to light gavaged with 9-*cis*-retinyl acetate (7.0 µmol) and kept in the dark before the retinoid analysis. 9-*cis*-Retinal (A, top) and 11-*cis*-retinal (A, bottom) levels were analyzed by HPLC as described under *Materials and Methods*. Mean ± S.D. was indicated (*n*= 3 for each point). Two days after 9-*cis*-retinyl acetate gavage, scotopic and photopic ERG was performed as described under *Materials and Methods*. Three mice from each group were examined, and representative scotopic waves were indicated (B).

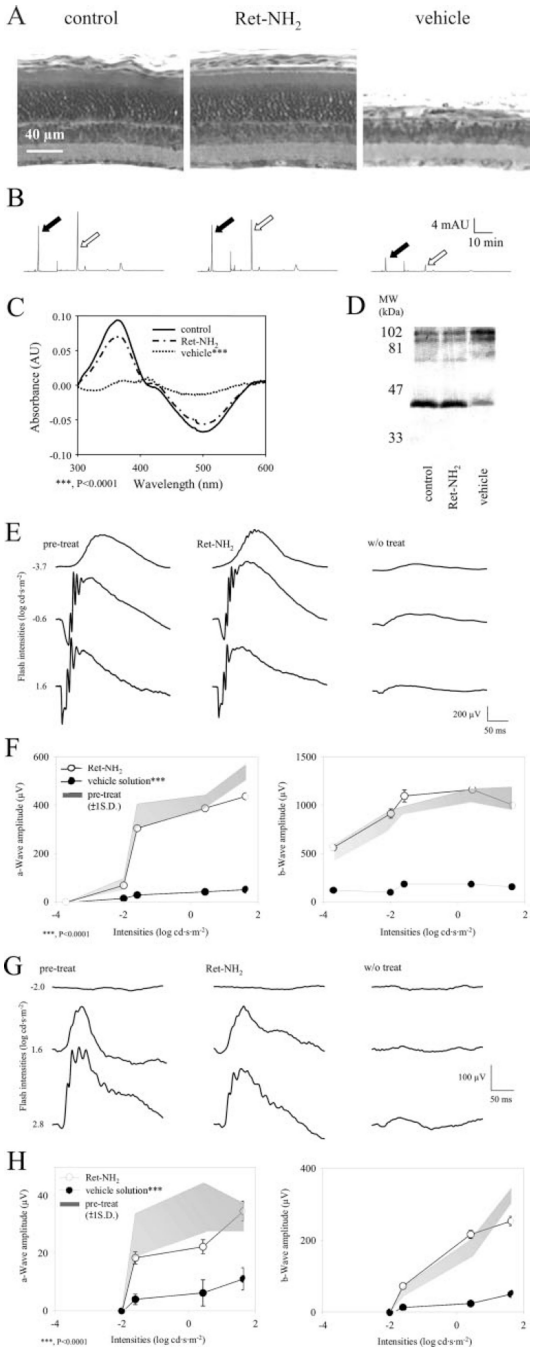

Fig. 7.

The protective effect of Ret-NH_2 on light-induced retinal damage in a mouse model. The 48-h dark-adapted BALB/c mice were gavaged once with Ret-NH_2 (3.5 μmol). After 16 h, mice were exposed to 5000 lux fluorescent light for 2 h to induce light damage of the retina. For the remaining time, mice were kept in the dark. A, morphology of the retina was examined 7 days after the light exposure. Left, the retina section from the control mouse not exposed to the intense light; middle, the retina section from mouse exposed to the intense light but treated with Ret-NH_2; right, the retina section from the control mouse exposed to the intense

light treated with vehicle solution only. Similar results were obtained from four independent experiments. B, retinoid content of the eyes from mice treated and exposed to light as in A. The eyes were analyzed for retinoid content 2 weeks after the light exposure as described under *Materials and Methods*. The black arrows indicate all-*trans*-retinyl ester, and the open arrows indicate 11-*cis*-retinal in the chromatograms of retinoid analysis. C, rhodopsin concentration was measured 2 weeks after the light exposure. D, immunoblot of rhodopsin from the light damage-induced mouse eyes with or without Ret-NH_2 treatment. Rhodopsin monomer and dimer were detected in control and Ret-NH_2 pretreated mice, whereas aggregated rhodopsin was detected in the mice treated with vehicle solution. E through H, mice were dark-adapted for 48 h, and scotopic (E, F) and photopic (G, H) ERG were recorded 7 days after light exposure as described under *Materials and Methods*. Ret-NH_2-treated mice showed no significant differences compared with the control, whereas the amplitudes in mice treated with vehicle solutions were attenuated significantly compared with control and Ret-NH_2-treated mice ($P < 0.0001$). Statistical analysis was performed by one-way analysis of variance ($n = 5$ in each condition).

TABLE 1

Retinoic acid production in the liver

Retinoids were analyzed as described under *Materials and Methods*.

Gavage	all-*trans* -Retinoic Acid							
	Not treated	**2h**	**4h**	**8h**	**24 h**	**72 h**	**1 wk**	**6 wk**
	pmol±S.D./125 mg liver							
Ret-NH_2 (1.75 μmol)	0 ± 0	0 ± 0	0 ± 0	0 ± 0	0 ± 0	0 ± 0	0 ± 0	
Ret-NH_2 (3.5 μmol)	0 ± 0	0 ± 0	0 ± 0	0 ± 0	0 ± 0	0 ± 0	0 ± 0	0 ± 0
Ret-NH_2 (17.5 μmol)	0 ± 0	2.8 ± 0.9	4.2 ± 1.2	3.4 ± 1.6	0 ± 0	0 ± 0	0 ± 0	
Fenretinide (17.5 μmol)	0 ± 0	6.8 ± 0.8	12.9 ± 0.67	4.6 ± 0.5	0 ± 0	0 ± 0		
all-*trans*-ROL (17.5 μmol)	0 ± 0	449.6 ± 37.9	1567.6 ± 565.4	54.9 ± 41.8	1.3 ±2.2	0 ± 0	0 ± 0	

TABLE 2

Rhodopsin amounts of LD (light-damaged) mice

Rhodopsin was analyzed as described under *Materials and Methods*.

	No Light	LD Induced	
		With Ret-NH_2	Without Ret-NH_2
Rhodopsin (pmol/eye)	476 ± 32	417 ± 55	82 ± 24*

*$P < 0.0001$.